International Journal of Applied Operational Research
Vol. 15, No. 1, pp. 1-25, Winter 2027

Journal homepage: ijorlu.liau.ac.ir

Robust multi-objective economic-statistical design of nonlinear profile monitoring under parameter uncertainty and multiple assignable causes: An MOGWO-based approach

H. Majdzangeneh, M. J. Ershadi*, M. R. Nabatchian

Received: 18 August 2026 ; **Accepted:** 2 October 2026

Abstract Monitoring nonlinear quality profiles becomes difficult when profile coefficients are correlated, several assignable causes may occur, and process and cost parameters are uncertain. This study develops a robust multi-objective economic-statistical design that integrates a third-order polynomial profile, an EWMA-Hotelling T^2 monitoring scheme, cause-specific competing risks, scenario-based parameter uncertainty, and a simulation-based regenerative cost model. The decision variables are sample size, sampling interval, control-limit multiplier, and EWMA smoothing parameter. Monte Carlo simulation is used to estimate in-control and out-of-control run-length behavior and calendar-time detection delay, while a constrained mixed-variable multi-objective grey wolf optimizer constructs feasible Pareto alternatives. The proposed search procedure is evaluated descriptively against NSGA-II and MOPSO under a matched verification setting. The results indicate that MOGWO provides a competitive balance between Pareto-front convergence and coverage, although competing algorithms retain advantages on individual diversity measures. Policy-level and sensitivity analyses further show that detection performance and economic cost are strongly influenced by process dispersion, shift magnitude, and out-of-control losses. The proposed framework provides practitioners with a transparent set of monitoring policies for balancing cost, false-alarm protection, detection speed, and robustness under uncertain operating conditions.

Keywords: Economic-Statistical Design, Statistical Process Control, EWMA-Hotelling T^2, Multi-Objective Grey Wolf Optimizer (MOGWO), Nonlinear Profile Monitoring, Parameter Uncertainty.

1 Introduction

Quality in many manufacturing and service processes is better represented by a functional relationship between a response and explanatory variables than by isolated measurements. Such relationships are monitored as quality profiles [1-4]. When the profile is nonlinear, an assignable cause may change level, slope, curvature, higher-order shape, or dispersion

*Corresponding Author. (✉)
E-mail: ershadi@irandoc.ac.ir (M.J. Ershadi)

H. Majdzangeneh
Department of Industrial Engineering, CT.C., Islamic Azad University, Tehran, Iran

M. J. Ershadi
Iranian Research Institute for Information Science and Technology (IranDoc), Tehran, Iran

M. R. Nabatchian
Department of Industrial Engineering, CT.C., Islamic Azad University, Tehran, Iran

[Downloaded from mail.ijaor.ir on 2026-11-25]

without creating a uniform deviation at every design point [2; 5-6]. Effective monitoring must therefore detect structural deterioration while controlling false alarms, sampling burden, and the economic consequences of delayed detection [3].

For polynomial nonlinear profiles, estimated coefficients are correlated and may change jointly. An EWMA-Hotelling T^2 scheme is attractive because it combines current and historical information while accounting for covariance among coefficient estimates [7-10]. Economic-statistical design is nevertheless difficult because a large in-control ARL, a small out-of-control ARL, and low long-run cost are conflicting objectives [11-15]. The problem becomes more realistic and more complex when sample size is integer, other design variables are continuous, several assignable causes have different rates and consequences, and process/cost parameters are uncertain [16-20].

Recent work has extended profile monitoring toward generalized-linear and functional profiles [20-25] and economic-statistical optimization toward uncertainty, multiple causes, memory-type charts, and multi-objective decision making [25-29]. However, these strands remain only partially integrated: nonlinear profile monitoring has mainly emphasized detection performance, whereas economic-statistical designs have predominantly focused on linear profiles or other chart families [30-32]. This motivates the research question addressed here: Can a single robust design jointly account for nonlinear coefficient changes, multiple assignable causes, parameter uncertainty, and economic-statistical trade-offs without reducing the decision to one scalar optimum?

The contribution of this study is therefore integrative rather than a claim that any individual component is new. Specifically, the framework (i) models a third-order nonlinear profile with cause-specific changes in coefficients and dispersion; (ii) monitors the correlated coefficient vector with a fixed-Phase-I EWMA-Hotelling T^2 scheme; (iii) evaluates run lengths, calendar-time delay, and long-run regenerative-cycle cost directly by Monte Carlo simulation under weighted uncertainty scenarios; and (iv) solves the resulting mixed integer-continuous three-objective problem with a feasibility-aware MOGWO archive, producing economic, statistical, false-alarm-protective, and balanced policies. This combination extends recent linear-profile and memory-type economic-statistical designs [33-34].

The manuscript is organized into five main sections: Introduction, Literature Review, Methodology, Findings, and Conclusion. A dedicated discussion subsection within the Findings section compares the results with prior studies and clarifies the scope of the evidence.

2 Literature review

Profile-monitoring research began with linear-profile methods and later expanded to nonlinear, generalized-linear, functional, and adaptive monitoring. Kang and Albin [12] and Woodall et al. [33] established the early profile-monitoring foundations, while Williams et al. [32] demonstrated multivariate monitoring of nonlinear profile parameters. More recent work has introduced variable-parameter statistical and machine-learning charts for generalized linear model profiles [23], robust multivariate functional monitoring [3], and broader syntheses of joint, double-sampling, and run-rule schemes [10, 11, 20]. These studies show a clear shift from isolated parameter surveillance toward adaptive monitoring of complex profile structures.

Economic-statistical research has progressed in parallel. Roshanbin et al. [22] used NSGA-II for a three-objective design of simple linear profiles, and Ershadi et al. [4] used

[Downloaded from mail.ijaor.ir on 2026-11-25]

MOPSO for linear profiles with multiple assignable causes. Shojaee et al. [29] incorporated parameter uncertainty into a Hotelling T^2 design, while recent studies have extended economic-statistical optimization to memory-type control charts with multiple causes Shiravani et al., [28], acceptance sampling Jafarian-Namin et al., [8], repetitive group sampling Jafarian-Namin et al., [9], p- and u-charts Sandeep & Mukhopadhyay [25], Sandeep & Mukhopadhyay [26], variable-sampling-interval EWMA charts Lee et al., [13], integrated production-maintenance monitoring Shojaee et al., [30], and risk-adjusted EWMA designs Nasiri Pour et al., [21]. These recent contributions reinforce the need to evaluate cost, false-alarm protection, detection performance, and operational constraints jointly.

Multi-objective metaheuristics are useful in this setting because the objectives are conflicting and the design space is mixed and simulation-based. MOGWO preserves non-dominated solutions in an external archive and selects multiple leaders to encourage coverage of the Pareto set [19-16]. Recent two-archive MOGWO developments further emphasize the importance of balancing convergence and diversity [31]. Nevertheless, algorithmic performance is problem-dependent; accordingly, this study compares MOGWO with NSGA-II and MOPSO under a common evaluator and does not assume superiority in advance.

The research gap lies at the intersection of these streams. Existing nonlinear-profile studies primarily address statistical detection, while economic-statistical profile designs remain concentrated on linear relationships; recent uncertainty-aware and multiple-cause studies do not simultaneously combine nonlinear profile changes, fixed Phase-I standardization, cause-specific competing risks, regenerative-cycle costing, and robust three-objective optimization. The present work addresses this gap by integrating these elements in one decision framework and by reporting not only Pareto-set quality but also representative policies, cost decomposition, and sensitivity to key economic and process parameters.

3 Methodology

This study develops an integrated, simulation-based, multi-objective approach for the economic-statistical design of nonlinear profile monitoring under parameter uncertainty. The statistical core of the approach estimates the coefficients of a third-order polynomial profile and jointly monitors them through an EWMA-Hotelling T^2 statistic [15-17-21]. The design parameters are the sample size, sampling interval, control-limit multiplier, and EWMA smoothing parameter. These parameters are optimized simultaneously with respect to three conflicting objectives: minimization of the robust long-run cost, maximization of the robust in-control average run length, and minimization of the robust out-of-control average run length. The economic structure follows the logic of economic-statistical control-chart design [22-25], but the cycle cost and run-length measures are evaluated directly by Monte Carlo simulation to accommodate the memory of the EWMA statistic and the presence of multiple assignable causes. The statistical formulation follows nonlinear profile monitoring [16] and the multivariate EWMA covariance treatment. The economic-cycle logic is consistent with classical economic-statistical design [18-20] and recent uncertainty and memory-type extensions [13, 28, 39].

The resulting optimization problem is solved using MOGWO [19, 16]. MOGWO maintains a fixed-size external archive of non-dominated solutions and selects leaders from less crowded regions of the objective space, thereby balancing convergence and diversity. Multiple assignable causes with different occurrence rates and shift patterns are incorporated, and the single-cause setting is recovered as the special case $K = 1$. The proposed

[Downloaded from mail.ijaor.ir on 2026-11-25]

implementation also fixes the Phase I reference covariance matrix during online monitoring; scenario-specific variances are used to generate observations but are not revealed to the control chart. This prevents the robust design from unrealistically assuming that the true operating scenario is known during Phase II.

3.1 Problem statement

At the beginning of each regenerative cycle, the process is assumed to be in control. After a random period, one of K assignable causes may occur and alter one or more profile coefficients, the error variance, or both. The process is sampled every h time units, and n observations are collected at predetermined design points during each sampling occasion. The coefficients of the current profile are estimated and monitored by an EWMA-Hotelling T^2 scheme. The monitoring policy is represented by the decision vector

$$\mathrm{d} = (n, h, L, r) \tag{1}$$

Here, n is the number of observations in each sampled profile, h is the time interval between consecutive samples, L is the control-limit multiplier, and r is the EWMA smoothing parameter. Increasing n generally improves coefficient estimation and change-detection capability but increases sampling cost. Reducing h may shorten the detection delay but increases sampling frequency. Increasing L reduces false alarms but can delay detection, while r controls the relative contribution of current and historical information. These relationships create an inherent conflict among the economic and statistical objectives, so the desired output is a set of Pareto-efficient monitoring policies rather than a single universally optimal solution.

For each candidate sample size, the explanatory-variable design points are taken as equally spaced values over a fixed operating interval $[x_{\min}, x_{\max}]$:

$$x_i = x_{\min} + \frac{i-1}{n-1}(x_{\max} - x_{\min}), \qquad i = 1,2,\dots,n. \tag{2}$$

This definition changes the number of observations when n changes without altering the physical operating range of the profile.

3.2 Architecture of the proposed approach

The proposed architecture consists of eight interconnected layers. The first layer specifies the profile structure, design points, in-control coefficients, and random-error model. The second defines the assignable causes and the effect of each cause on the profile coefficients and process dispersion. The third estimates the Phase I reference mean vector and covariance matrix. The fourth constructs the Phase II EWMA-Hotelling T^2 monitoring statistic. The fifth generates uncertainty scenarios for the economic and process parameters. The sixth evaluates each monitoring policy under every scenario through Monte Carlo simulation. The seventh aggregates scenario-dependent outcomes into robust economic and statistical measures. Finally, the eighth uses MOGWO to search the decision space and construct an external archive of feasible non-dominated policies. Operationally, each grey wolf represents a complete monitoring policy. For every candidate policy, in-control and out-of-control profiles are generated, the profile coefficients are estimated, the EWMA statistic is updated, and the first signaling time is recorded. The evaluation is repeated for all assignable causes, uncertainty scenarios, and simulation replications. The resulting cost, ARL_0, and ARL_1 values

[Downloaded from mail.ijaor.ir on 2026-11-25]

are returned to MOGWO as objective-function values. After each generation, the external archive is updated so that only feasible, non-dominated, and sufficiently diverse solutions are retained.

3.3 Model assumptions

The process begins in the in-control state after each repair or adjustment. The quality profile is represented by a third-order polynomial. The response curve is nonlinear with respect to the explanatory variable x, although it is linear in the regression coefficients. Within each scenario, the random errors are assumed to be independent and normally distributed with zero mean. A set of historical in-control profiles is available in Phase I for estimating the fixed reference parameters, while new profiles are sequentially monitored in Phase II. The model allows K independent competing assignable causes. Each cause may have a distinct occurrence rate, shift vector, out-of-control production cost, search time, and repair time. The causes compete only while the process is in control. Once the first cause occurs, no additional cause is assumed to occur until the existing cause is detected and removed, which allows each regenerative cycle to be associated with a unique cause [28]. Following a false alarm, the process is investigated and, if no assignable cause is confirmed, the EWMA vector is reset to the Phase I reference mean before monitoring resumes. The same reset is applied after a true signal and process repair. The sample size n is an integer decision variable, whereas h, L, and r are continuous decision variables.

3.4 Nonlinear profile model

For profile j, the response observed at design point i is represented by the third-order polynomial model [32]:

$$y_{ij} = \beta_{0j} + \beta_{1j}x_i + \beta_{2j}x_i^2 + \beta_{3j}x_i^3 + \varepsilon_{ij}, \qquad i = 1,2,\dots,n. \tag{3}$$

In Equation (3), y_{ij} is the observed response, x_i is the explanatory-variable value, and $\beta_{0j},\dots,\beta_{3j}$ are the coefficients of profile j. Under uncertainty scenario s, the random error used to generate observations satisfies

$$\varepsilon_{ij,s} \sim N(0,\sigma_s^2). \tag{4}$$

The in-control coefficient vector is:

$$\beta = (\beta_0,\beta_1,\beta_2,\beta_3)^T. \tag{5}$$

If assignable cause k occurs under scenario s, its shift vector is:

$$\delta_{k,s} = \left(\delta_{0k,s},\delta_{1k,s},\delta_{2k,s},\delta_{3k,s}\right)^T. \tag{6}$$

The corresponding out-of-control coefficient vector is:

$$\beta_{k,s}^* = \beta + \delta_{k,s}. \tag{7}$$

The shift vector may affect one coefficient or any combination of coefficients. A change in β_0 shifts the overall profile level, a change in β_1 modifies the slope, and changes in β_2 or β_3 alter curvature and higher-order shape. When dispersion changes are also considered, the shifted standard deviation is:

$$\sigma_{k,s}^* = \rho_{\sigma,k,s}\,\sigma_s \tag{8}$$

where $\rho_{\sigma,k,s}$ is the dispersion multiplier associated with cause k in scenario s.

[Downloaded from mail.ijaor.ir on 2026-11-25]

3.5 Estimation of the profile coefficients

For a profile containing n observations, the design matrix is

$$\mathrm{X} = \begin{bmatrix} 1 & x_1 & x_1^2 & x_1^3 \\ 1 & x_2 & x_2^2 & x_2^3 \\ \vdots & \vdots & \vdots & \vdots \\ 1 & x_n & x_n^2 & x_n^3 \end{bmatrix}. \tag{9}$$

The response vector of profile j is:

$$\mathrm{y}_j = \left(y_{1j}, y_{2j}, \dots, y_{nj}\right)^T. \tag{10}$$

The least-squares estimator of the coefficient vector is:

$$\hat{\beta}_j = (\mathrm{X}^T\mathrm{X})^{-1}\mathrm{X}^T\mathrm{y}_j. \tag{11}$$

Using m_0 historical in-control profiles, the Phase I reference mean vector is estimated as:

$$\hat{\mu}_\beta = \frac{1}{m_0}\sum_{j=1}^{m_0}\hat{\beta}_j. \tag{12}$$

The corresponding Phase I covariance estimator is:

$$\hat{\Sigma}_\beta = \frac{1}{m_0 - 1}\sum_{j=1}^{m_0}\left(\hat{\beta}_j - \hat{\mu}_\beta\right)\left(\hat{\beta}_j - \hat{\mu}_\beta\right)^T. \tag{13}$$

The covariance structure is retained because the polynomial coefficient estimators are generally correlated. Importantly, $\hat{\mu}_\beta$ and $\hat{\Sigma}_\beta$ remain fixed during Phase II. Scenario-specific values of σ_s affect the generated observations but are not used to re-standardize the chart online.

3.6 EWMA-Hotelling T² Monitoring Statistic

The EWMA vector for profile j is updated as (Lowry et al., 1992)

$$\mathrm{M}_j = r\hat{\beta}_j + (1-r)\mathrm{M}_{j-1}, \qquad 0 < r < 1. \tag{14}$$

The initial vector is set equal to the Phase I reference mean:

$$\mathrm{M}_0 = \hat{\mu}_\beta. \tag{15}$$

To account for start-up behavior, the time-dependent covariance matrix is:

$$\Sigma_{M,j} = \frac{r}{2-r}\left[1 - (1-r)^{2j}\right]\hat{\Sigma}_\beta. \tag{16}$$

The monitoring statistic is:

$$T_j^2 = \left(\mathrm{M}_j - \hat{\mu}_\beta\right)^T\Sigma_{M,j}^{-1}\left(\mathrm{M}_j - \hat{\mu}_\beta\right). \tag{17}$$

The upper control limit is specified by:

$$H = L\,\chi^2_{p,1-\alpha}, \tag{18}$$

Where p is the number of monitored coefficients, $\chi^2_{p,1-\alpha}$ is a reference chi-square quantile, and L is an optimizable scaling coefficient. For the third-order polynomial, $p = 4$. Because successive EWMA statistics are temporally dependent, the actual in-control run-length performance associated with a candidate value of L is determined by simulation rather than directly from α. The chart signals when:

$$T_j^2 \geq H. \tag{19}$$

[Downloaded from mail.ijaor.ir on 2026-11-25]

3.7 Statistical performance measures

The run length is the number of sampled profiles observed from the beginning of monitoring until the first signal. For scenario s and policy d, the in-control average run length is:

$$ARL_0(s,\mathrm{d}) = E[RL \mid IC, s, \mathrm{d}]. \quad (20)$$

For assignable cause k, the out-of-control average run length is

$$ARL_{1,k}(s,\mathrm{d}) = E[RL \mid k, s, \mathrm{d}]. \quad (21)$$

For each policy and scenario, B_0 in-control sequences and B_1 out-of-control sequences are generated. The Monte Carlo estimators are:

$$\widehat{ARL}_0(s,\mathrm{d}) = \frac{1}{B_0}\sum_{b=1}^{B_0} R\, L_{0,b}(s,\mathrm{d}), \quad (22)$$

and

$$\widehat{ARL}_{1,k}(s,\mathrm{d}) = \frac{1}{B_1}\sum_{b=1}^{B_1} R\, L_{1,b,k}(s,\mathrm{d}). \quad (23)$$

Because h is a decision variable, policies with similar ARL_1 values may have different calendar-time detection delays. Therefore, the cause-specific delay is additionally reported as:

$$Delay_k(s,\mathrm{d}) = E\left[T_{\mathrm{signal}} - T_{\mathrm{shift}} \mid k, s, \mathrm{d}\right]. \quad (24)$$

3.8 Multiple assignable causes

The K assignable causes are modeled as competing risks. Let $\theta_{k,s}$ denote the occurrence rate of cause k in scenario s. The total transition rate from the in-control state is:

$$\Theta_s = \sum_{k=1}^{K} \theta_{k,s}. \quad (25)$$

The in-control operating time follows:

$$\tau_s \sim \mathrm{Exp}(\Theta_s). \quad (26)$$

Conditional on an assignable cause occurring, the probability that cause k occurs first is:

$$\pi_{k,s} = \frac{\theta_{k,s}}{\Theta_s}. \quad (27)$$

These probabilities are used to aggregate cause-specific performance. The scenario-specific out-of-control average run length is:

$$ARL_1(s,\mathrm{d}) = \sum_{k=1}^{K} \pi_{k,s}\, ARL_{1,k}(s,\mathrm{d}), \quad (28)$$

and the scenario-specific calendar-time detection delay is:

$$Delay(s,\mathrm{d}) = \sum_{k=1}^{K} \pi_{k,s}\, Delay_k(s,\mathrm{d}). \quad (29)$$

3.9 Simulation-based economic cycle model

A regenerative cycle starts when the repaired process returns to the in-control state and ends when an assignable cause has been detected, investigated, and repaired. The total cycle cost

[Downloaded from mail.ijaor.ir on 2026-11-25]

includes in-control production cost, out-of-control production loss, false-alarm cost, search-and-repair cost, and sampling cost. For simulation replication ℓ in scenario s, let k_ℓ denote the cause that occurs during that cycle. The total cycle cost is:

$$TC_{\ell,s}(\mathrm{d}) = \quad C_{0,s}T_{IC,\ell,s} + C_{1,k_\ell,s}T_{OOC,\ell,s} + F_s N_{FA,\ell,s} + W_{k_\ell,s} + (a_s + c_s n)N_{S,\ell,s}. \tag{30}$$

Here, $C_{0,s}$ is the in-control production-cost rate, $C_{1,k,s}$ is the out-of-control production-cost rate associated with cause k, T_{IC} and T_{OOC} are the in-control and out-of-control operating times, F_s is the cost of one false alarm, N_{FA} is the number of false alarms, $W_{k,s}$ is the search-and-repair cost, a_s is the fixed sampling cost, c_s is the variable cost per observation, and N_S is the number of sampled profiles. The corresponding cycle length is:

$$TL_{\ell,s}(\mathrm{d}) = \quad T_{IC,\ell,s} + T_{OOC,\ell,s} + N_{FA,\ell,s}T_{FA,s} + T_{search,k_\ell,s} + T_{repair,k_\ell,s} + I_{stop}\, N_{S,\ell,s}E(n) \tag{31}$$

Where $I_{stop} = 1$ when sampling interrupts production and $I_{stop} = 0$ otherwise, and $E(n)$ is the time required to collect and estimate one profile. The long-run cost per unit time is estimated by the ratio of total simulated costs to total simulated cycle lengths:

$$C_s(\mathrm{d}) = \frac{\sum_{\ell=1}^{B_C} T\, C_{\ell,s}(\mathrm{d})}{\sum_{\ell=1}^{B_C} T\, L_{\ell,s}(\mathrm{d})}. \tag{32}$$

This formulation directly incorporates the memory behavior of the EWMA chart, the realized shift time, the observed number of false alarms, and the actual detection delay into the economic evaluation.

3.10 Uncertainty modeling and robust measures

The uncertainty set contains S weighted scenarios with:

$$w_s \geq 0, \qquad \sum_{s=1}^{S} w_s = 1. \tag{33}$$

The uncertain parameters may include assignable-cause rates, out-of-control production costs, false-alarm costs, repair costs, sampling costs, process standard deviation, and shift magnitudes. A generic uncertain parameter is generated as:

$$q_s = q_0(1 + \rho_s), \tag{34}$$

where q_0 is the nominal value and ρ_s is the scenario-specific relative perturbation. The perturbation intervals are selected so that all rates, costs, durations, and standard deviations remain strictly positive. Scenarios may be generated by Latin hypercube sampling over pre specified uncertainty intervals. For any scenario-dependent performance measure $g_s(\mathrm{d})$, the weighted mean and standard deviation are In the numerical study, the uncertainty design uses three equally weighted scenarios (w_s = 1/3): the nominal configuration and Latin-hypercube perturbations. The perturbation ranges are sigma ±5%; cause-specific coefficient shifts and occurrence rates ±10%; C1 ±15%; and the remaining cost and time parameters ±10% (Table 1). Equal weights are used because no empirical scenario probabilities are available; the robust objectives therefore represent an equiprobable stress-test design rather than a fitted probabilistic forecast. The same scenario set and weights are used for all algorithms.

$$\mu_g(\mathrm{d}) = \sum_{s=1}^{S} w_s\, g_s(\mathrm{d}), \tag{35}$$

and

[Downloaded from mail.ijaor.ir on 2026-11-25]

$$\sigma_g(\mathrm{d}) = \sqrt{\sum_{s=1}^{S} w_s \left[g_s(\mathrm{d}) - \mu_g(\mathrm{d})\right]^2}. \quad (36)$$

The robust economic objective is:

$$RCost(\mathrm{d}) = \mu_C(\mathrm{d}) + \lambda_C \sigma_C(\mathrm{d}). \quad (37)$$

Because a larger ARL_0 is desirable, its conservative robust measure is:

$$RARL_0(\mathrm{d}) = \mu_{ARL_0}(\mathrm{d}) - \lambda_0 \sigma_{ARL_0}(\mathrm{d}). \quad (38)$$

For the cause-weighted ARL_1, define:

$$\mu_{ARL_1}(\mathrm{d}) = \sum_{s=1}^{S} w_s\, ARL_1(s, \mathrm{d}), \quad (39)$$

$$\sigma_{ARL_1}(\mathrm{d}) = \sqrt{\sum_{s=1}^{S} w_s \left[ARL_1(s, \mathrm{d}) - \mu_{ARL_1}(\mathrm{d})\right]^2}, \quad (40)$$

and

$$RARL_1(\mathrm{d}) = \mu_{ARL_1}(\mathrm{d}) + \lambda_1 \sigma_{ARL_1}(\mathrm{d}). \quad (41)$$

To protect against poor performance for an individual cause, the cause-specific robust measures are also defined:

$$\mu_{ARL_{1,k}}(\mathrm{d}) = \sum_{s=1}^{S} w_s\, ARL_{1,k}(s, \mathrm{d}), \quad (42)$$

$$\sigma_{ARL_{1,k}}(\mathrm{d}) = \sqrt{\sum_{s=1}^{S} w_s \left[ARL_{1,k}(s, \mathrm{d}) - \mu_{ARL_{1,k}}(\mathrm{d})\right]^2}, \quad (43)$$

and

$$RARL_{1,k}(\mathrm{d}) = \mu_{ARL_{1,k}}(\mathrm{d}) + \lambda_1 \sigma_{ARL_{1,k}}(\mathrm{d}). \quad (44)$$

Calendar-time delay is retained as a supplementary robust measure:

$$RDelay(\mathrm{d}) = \mu_{Delay}(\mathrm{d}) + \lambda_D \sigma_{Delay}(\mathrm{d}). \quad (45)$$

The coefficients λ_C, λ_0, λ_1, and λ_D represent risk-aversion levels. A zero value yields mean-based evaluation, while larger values place more emphasis on stability across uncertainty scenarios.

3.11 Multi-objective mathematical formulation

The proposed model contains three objective functions:

$$\min f_1(\mathrm{d}) = RCost(\mathrm{d}), \quad (46)$$

$$\min f_2(\mathrm{d}) = -RARL_0(\mathrm{d}), \quad (47)$$

and

$$\min f_3(\mathrm{d}) = RARL_1(\mathrm{d}). \quad (48)$$

The negative sign in Equation (47) converts maximization of robust in-control protection into minimization form. The statistical constraints are:

$$RARL_0(\mathrm{d}) \geq ARL_{0,\min}, \quad (49)$$

and

[Downloaded from mail.ijaor.ir on 2026-11-25]

$$RARL_{1,k}(\mathrm{d}) \le ARL_{1,\max}, \qquad k = 1,2,\dots,K. \tag{50}$$

The decision-variable bounds are:

$$n_{\min} \le n \le n_{\max}, \qquad n \in \mathbb{N}, \tag{51}$$

$$h_{\min} \le h \le h_{\max}, \tag{52}$$

$$L_{\min} \le L \le L_{\max}, \tag{53}$$

and

$$0 < r_{\min} \le r \le r_{\max} < 1. \tag{54}$$

For comparability with the baseline study, preliminary bounds of $5 \le n \le 20$, $0.5 \le h \le 12$, $0.6 \le L \le 2$, and $0.05 \le r \le 0.80$ may be used. Final bounds should be confirmed through pilot experiments and application-specific considerations.

3.12 Constraint handling

For better justification of optimization model (which has been described in section 3.11) a constraint handling method is applied. In this model, between two feasible solutions, Pareto dominance is implemented using the three objective functions. Between two infeasible solutions, the solution with the smaller normalized constraint violation is preferred. The total violation is

$$CV(\mathrm{d}) = \max\left\{0, \frac{ARL_{0,\min} - RARL_0(\mathrm{d})}{ARL_{0,\min}}\right\} + \sum_{k=1}^{K} \max\left\{0, \frac{RARL_{1,k}(\mathrm{d}) - ARL_{1,\max}}{ARL_{1,\max}}\right\}. \tag{55}$$

3.13 Multi-Objective Grey Wolf Optimizer (MOGWO)

MOGWO extends the leadership and encircling mechanisms of the original Grey Wolf Optimizer Mirjalili et al., [19] to multi-objective problems through an external archive and density-based leader selection [19-16]. Each wolf represents one monitoring policy, $\mathrm{X}_i = (n_i, h_i, L_i, r_i)$. At iteration t, the exploration-exploitation parameter decreases linearly:

$$a_t = 2 - \frac{2t}{T_{\max}}. \tag{56}$$

For each leader $m \in \{\alpha, \beta, \delta\}$, the coefficient vectors are:

$$\mathrm{A}_m = 2a_t \mathrm{u}_{1,m} - a_t, \tag{57}$$

and

$$\mathrm{C}_m = 2\mathrm{u}_{2,m}, \tag{58}$$

where $\mathrm{u}_{1,m}$ and $\mathrm{u}_{2,m}$ are independent random vectors uniformly distributed over $[0,1]$. The distance from wolf i to leader m and the corresponding candidate position are:

$$\mathrm{D}_m = |\mathrm{C}_m \odot \mathrm{X}_m - \mathrm{X}_i|, \tag{59}$$

and

$$\mathrm{Y}_m = \mathrm{X}_m - \mathrm{A}_m \odot \mathrm{D}_m, \tag{60}$$

where $\odot$ denotes element-wise multiplication. The updated position is:

$$\mathrm{X}_i(t+1) = \frac{\mathrm{Y}_\alpha + \mathrm{Y}_\beta + \mathrm{Y}_\delta}{3}. \tag{61}$$

After the update, continuous variables are clipped to their feasible intervals, and the integer sample-size variable is repaired as:

[Downloaded from mail.ijaor.ir on 2026-11-25]

$$n_i \leftarrow \text{round}\left[\min\left(n_{\max}, \max(n_{\min}, n_i)\right)\right]. \quad (62)$$

3.14 External archive and leader selection

After each generation, the current population and archive are merged, dominated solutions are removed, and the remaining non-dominated solutions are stored in a fixed-size external archive. The objective space is partitioned into grid cells. The following normalized density-based probabilities constitute the archive-management adaptation used in this study. A leader is selected from occupied cell j with probability

$$P_{select}(j) = \frac{N_j^{-\eta}}{\sum_{l=1}^{G} N_l^{-\eta}}, \quad (63)$$

where N_j is the number of archived solutions in cell j, G is the number of occupied cells, and η controls leader-selection pressure. When the archive exceeds its maximum capacity, a crowded cell is selected for deletion with probability

$$P_{delete}(j) = \frac{N_j^{\zeta}}{\sum_{l=1}^{G} N_l^{\zeta}}. \quad (64)$$

This density-based mechanism prevents the archive from collapsing into a narrow region of the Pareto frontier and maintains a well-distributed set of trade-off solutions.

3.15 Computational procedure

The computational procedure begins by specifying the model parameters, decision-variable bounds, uncertainty scenarios, population size, archive capacity, and stopping criterion. An initial grey-wolf population is generated randomly, and the integer variable n is repaired. Each policy is evaluated under all uncertainty scenarios through Monte Carlo simulation, after which the three objective values and the constraint violation are calculated. The nondominated solutions are inserted into the external archive, three leaders are selected from sparsely populated cells, and wolf positions are updated according to Equations (56)-(61). Evaluation, archiving, leader selection, and updating continue until the maximum number of generations or objective-function evaluations is reached. Because the objective functions are simulation-based, common random numbers are used to reduce noise in policy comparisons. A moderate number of replications is used during optimization to control computational time. After the final archive is constructed, all selected solutions are re-evaluated using a substantially larger number of replications. A policy is retained in the final Pareto set only if its statistical constraints remain satisfied under high-precision validation.

3.16 Validation, statistical testing, and computational cost assessment

The proposed algorithm is compared with NSGA-II and MOPSO under a common simulation evaluator. The reported verification configuration uses the same decision bounds, uncertainty scenarios and weights, statistical constraints, Monte Carlo replication settings, population

[Downloaded from mail.ijaor.ir on 2026-11-25]

size, stopping rule, objective-function evaluation budget, feasibility-based constraint handling, and matched random-number streams for all three algorithms (Table 2). No algorithm-specific tuned advantage is claimed; the retained package does not contain a separate tuning log, so the comparison is explicitly treated as verification-level evidence. The current evidence contains one independent run per algorithm. Therefore, the HV, IGD+, Spacing, and Spread values are interpreted descriptively and are not used to claim statistically significant superiority. For a confirmatory study, each algorithm should be executed independently 30 times with matched seeds; each quality metric should then be analyzed using a Friedman omnibus test followed, when appropriate, by Holm-adjusted paired Wilcoxon signed-rank comparisons, with medians, interquartile ranges, and effect sizes reported [14].

Computational cost is dominated by the Monte Carlo evaluator rather than by the position update of the metaheuristic. Let N_eval denote the number of candidate policies evaluated, S the number of scenarios, m the number of assignable causes, and B0, B1, and BC the replication counts used for in-control, out-of-control, and regenerative-cycle simulation. The leading simulation cost scales as O (N_eval S [B0 E(RL0) + sum_c B1 E(RL1,c) + BC E(Ncycle)] Cprofile), where Cprofile is the cost of generating and fitting one profile and updating the EWMA statistic. With four polynomial coefficients, Cprofile is dominated by small least-squares and covariance operations and is modest relative to long run-length simulation. Archive dominance and density operations add at most quadratic overhead in population/archive size per generation. Wall-clock timing logs were not retained for the verified run; accordingly, no unsupported runtime values are reported, and practical runtime comparison is identified as part of the 30-run confirmatory experiment.

3.17 Final policy selection and methodological contribution

The primary output of the proposed model is a set of Pareto-efficient monitoring policies rather than a single solution. For managerial interpretation, at least three representative policies are reported: an economic policy with the smallest robust cost, a statistical policy with the smallest robust ARL_1, and a balanced policy corresponding to the knee point of the Pareto frontier. The knee point identifies a solution beyond which a small improvement in one objective requires a substantial deterioration in one or more competing objectives. Calendar-time detection delay is also reported for these representative policies to clarify their practical response speed. The methodological contribution of the proposed approach lies in the joint integration of nonlinear profile monitoring, multiple assignable causes, scenario-based parameter uncertainty, direct simulation of a memory-type EWMA scheme, and mixed-variable multi-objective optimization using MOGWO. The resulting approach provides a risk-aware decision-support tool for balancing monitoring cost, false-alarm protection, change-detection speed, and performance stability under uncertain industrial conditions.

4 Findings

This section evaluates the proposed approach from four complementary perspectives: the ability to represent heterogeneous nonlinear changes, the quality of the generated Pareto approximation, the comparative behavior of MOGWO against NSGA-II and MOPSO, and the economic and statistical robustness of representative monitoring policies. All three algorithms

[Downloaded from mail.ijaor.ir on 2026-11-25]

used the same simulation evaluator, uncertainty scenarios, feasibility rules, objective definitions, and evaluation budget; therefore, observed differences originate from the search mechanisms rather than from unequal problem formulations.

The numerical evidence reported below corresponds to the verified preliminary configuration used to test the complete computational pipeline. One independent run per algorithm is available in the retained evidence. Consequently, the figures and set-quality metrics are treated as descriptive verification results only; they do not establish statistically significant or universal algorithmic superiority. The repeated-run statistical protocol required for inferential comparison is defined in Section 3 and is reserved for the confirmatory experiment.

4.1 Experimental design and reproducibility

The nominal in-control profile was defined by the coefficient vector (3.00, 1.50, -0.80, 0.35) over the fixed design interval [0, 1]. Three assignable causes were considered. The first cause primarily shifted the profile level, the second altered the slope and curvature, and the third combined coefficient changes with a 15% increase in process dispersion. This structure deliberately avoids treating all out-of-control states as a single generic shift. Instead, it tests whether the monitoring policy remains effective when the direction and severity of the nonlinear change differ across causes. Such heterogeneity is central to the proposed contribution because earlier economic-statistical profile models were predominantly developed for simple linear profiles or a single representative shift [4, 22, 39].

Table 1 Numerical example with determined parameters for applied control chart and cost function

Item	Value
In-control coefficient vector	(3.00, 1.50, -0.80, 0.35)
Nominal process standard deviation	0.35
Cause 1 coefficient shift	(0.12, 0.00, 0.00, 0.00)
Cause 2 coefficient shift	(0.00, 0.12, -0.08, 0.04)
Cause 3 coefficient shift	(0.00, 0.08, 0.05, -0.03)
Dispersion multipliers	(1.00, 1.00, 1.15)
Assignable-cause rates	(0.0015, 0.0013, 0.0012)
In-control cost rate	10
Out-of-control cost rates	(105, 125, 150)
False-alarm cost	450
Search and repair costs	(1100, 1200, 1400)
Fixed / per-observation sampling costs	20 / 4
Scenario structure	Nominal scenario plus Latin-hypercube perturbations
Uncertainty ranges	sigma ±5%; shifts and rates ±10%; C1 ±15%; other costs/times ±10%

[Downloaded from mail.ijaor.ir on 2026-11-25]

Table 2 Decision variables and computational settings

Setting	Value
Decision vector	d = (n, h, L, r)
Sample-size bound	$5 \le n \le 20$; integer
Sampling-interval bound	$0.5 \le h \le 12$
Control-limit multiplier	$0.6 \le L \le 2.0$
EWMA smoothing parameter	$0.05 \le r \le 0.80$
Statistical constraints	RARL0 ≥ 200; cause-specific RARL1 ≤ 50
Uncertainty scenarios	3 equally weighted scenarios
Monte Carlo replications	B0 = 50; B1 = 40; BC = 20
Population / generations	12 / 6
Archive capacity / grid divisions	40 / 8
Independent runs in current evidence	1 per algorithm
Random-number control	Common random numbers and matched seeds
Stopping criterion	Six generations with a matched objective-function evaluation budget
Constraint handling	Feasibility-based dominance; normalized violation in Eq. (55)
Algorithm-specific tuning	No tuned-superiority claim; a separate tuning log is not retained in the verification package
Confirmatory statistical protocol	30 matched-seed runs; Friedman test + Holm-adjusted paired Wilcoxon tests; median/IQR/effect sizes
Runtime reporting	Analytical complexity reported; wall-clock logs unavailable for the retained verification run

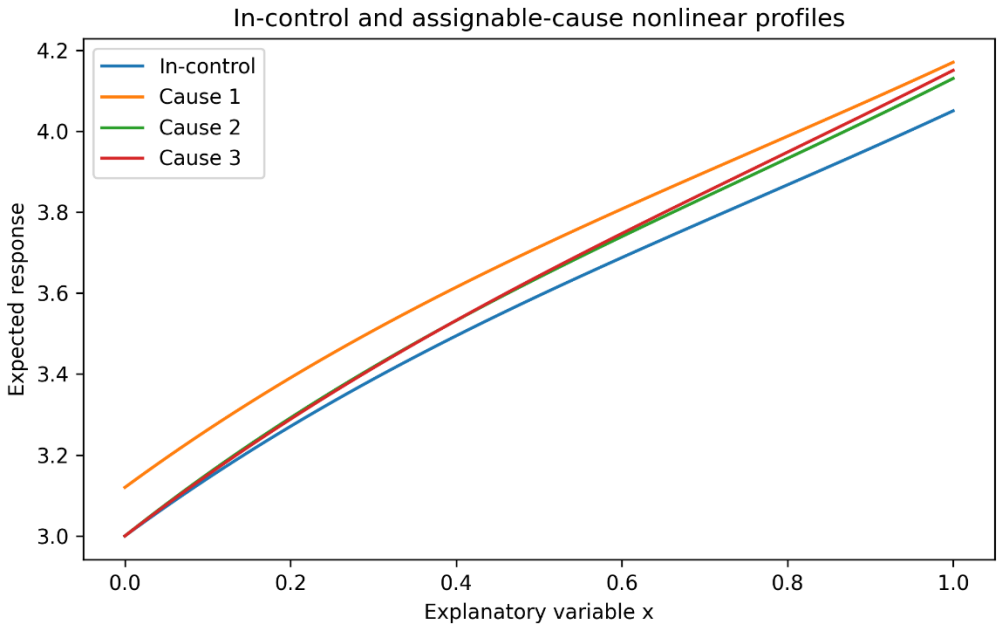

Fig. 1 In-control profile and three different cause-specific nonlinear profile

Figure 1 shows that the assignable causes are not simple parallel translations of the same curve. The separation between the in-control and out-of-control profiles varies across the design interval, which changes the information content of individual observations and requires joint monitoring of the estimated coefficient vector. The figure therefore illustrates why a multivariate EWMA-Hotelling T^2 statistic is more appropriate than independent univariate charts for the coefficients. It also demonstrates the practical importance of cause-specific ARL constraints: a policy with acceptable average detection performance can still react slowly to one particular change pattern unless each cause is explicitly examined.

[Downloaded from mail.ijaor.ir on 2026-11-25]

4.2 Pareto-front structure and objective trade-offs

The optimization problem contains three conflicting objectives: robust cost and robust ARL1 are minimized, whereas robust ARL0 is maximized. A solution with a very low cost is not necessarily desirable if it operates close to the minimum ARL0 constraint or fails to protect the process from frequent false alarms. Conversely, an extremely conservative control limit can generate a very large ARL0 while increasing detection delay and out-of-control losses. The relevant output is therefore a set of non-dominated policies rather than a single optimum. MOGWO, NSGA-II, and MOPSO were evaluated under identical conditions so that their ability to cover this trade-off surface could be assessed fairly. MOGWO uses a fixed-size archive and multiple leaders selected from less crowded objective-space regions [19], whereas NSGA-II relies on non-dominated sorting and crowding distance and MOPSO uses a repository-guided swarm search. These structural differences are directly reflected in the shape and coverage of the approximation sets.

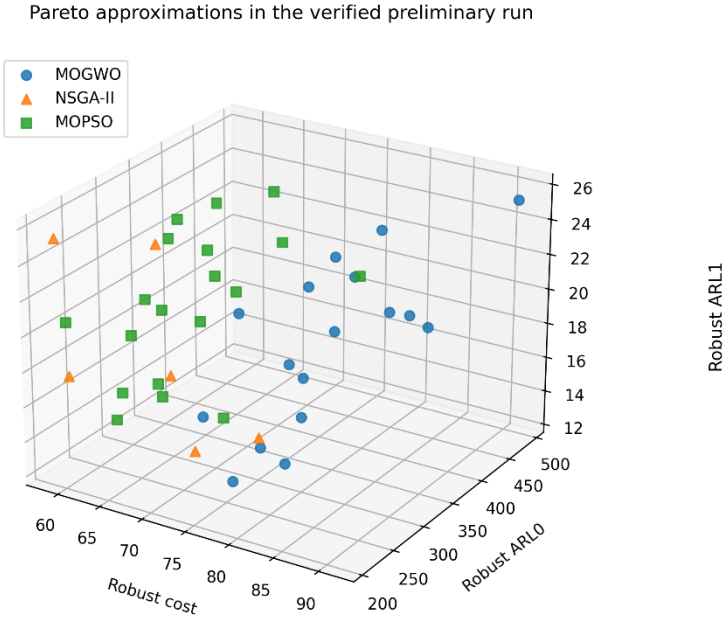

Fig. 2 Optimized Pareto solutions in three different dimensions

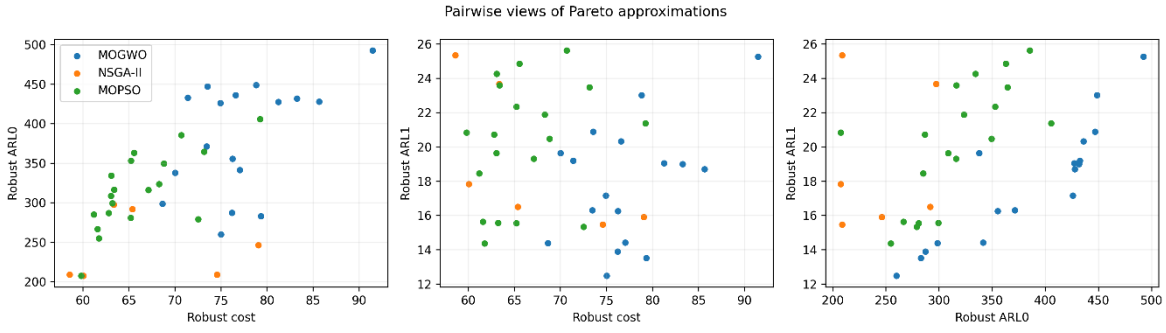

Fig. 3 Pairwise view of Pareto optimized solutions

Figures 2 and 3 reveal three important patterns. First, the feasible solutions form an extended trade-off surface rather than a compact cluster, confirming that cost, false-alarm protection, and detection speed cannot be optimized independently. Second, the MOGWO

[Downloaded from mail.ijaor.ir on 2026-11-25]

solutions cover a comparatively broad region of the objective space, including policies with high ARL0 as well as policies with low ARL1. This coverage is consistent with the use of density-based leader selection and archive management; whose purpose is to avoid concentration around a narrow portion of the Pareto frontier. Third, NSGA-II reaches a low-cost extreme in the preliminary run, but its feasible approximation contains substantially fewer points and covers a narrower range of ARL0 values. MOPSO produces a dense and relatively uniform set, but its approximation is generally closer to MOGWO than to NSGA-II in set-quality terms. The figures therefore indicate that the main advantage of MOGWO is not the production of a single cheapest solution; rather, it is the generation of a richer and more decision-relevant set of efficient alternatives.

4.3 Comparative algorithmic performance

Set-level performance was assessed using Hyper volume, IGD+, Spacing, and Spread. Hyper volume measures the dominated portion of the normalized objective space and rewards both convergence and coverage [12]. IGD+ evaluates the distance from a reference approximation to the obtained solution set while respecting Pareto dominance [17]. Lower Spacing values indicate a more uniform distribution among neighboring solutions, whereas larger Spread values indicate wider coverage of the feasible trade-off surface. Feasibility rate and archive size were also reported because a high-quality approximation is not useful if statistical constraints are violated or if only a few alternatives are retained. Recent MOGWO benchmarking likewise uses Hyper volume, generational-distance measures, spacing, and Friedman ranking to evaluate convergence and diversity jointly [31].

Table 3 A comparative study on three optimization methods applied to proposed multi-objective economic-statistical model

Algorithm	HV ↑	IGD+ ↓	Spacing ↓	Spread ↑	Feasible solutions	Interpretation
MOGWO	0.6323	0.0861	0.0990	0.8273	17	Best observed Hypervolume, IGD+, and Spread in the verified run; broad feasible coverage
NSGA-II	0.3109	0.2459	0.0864	0.5629	6	Lowest observed cost extreme in the verified run, but narrow set coverage
MOPSO	0.5255	0.0957	0.0630	0.7139	19	Best observed Spacing and largest feasible archive; competitive set quality in the verified run

[Downloaded from mail.ijaor.ir on 2026-11-25]

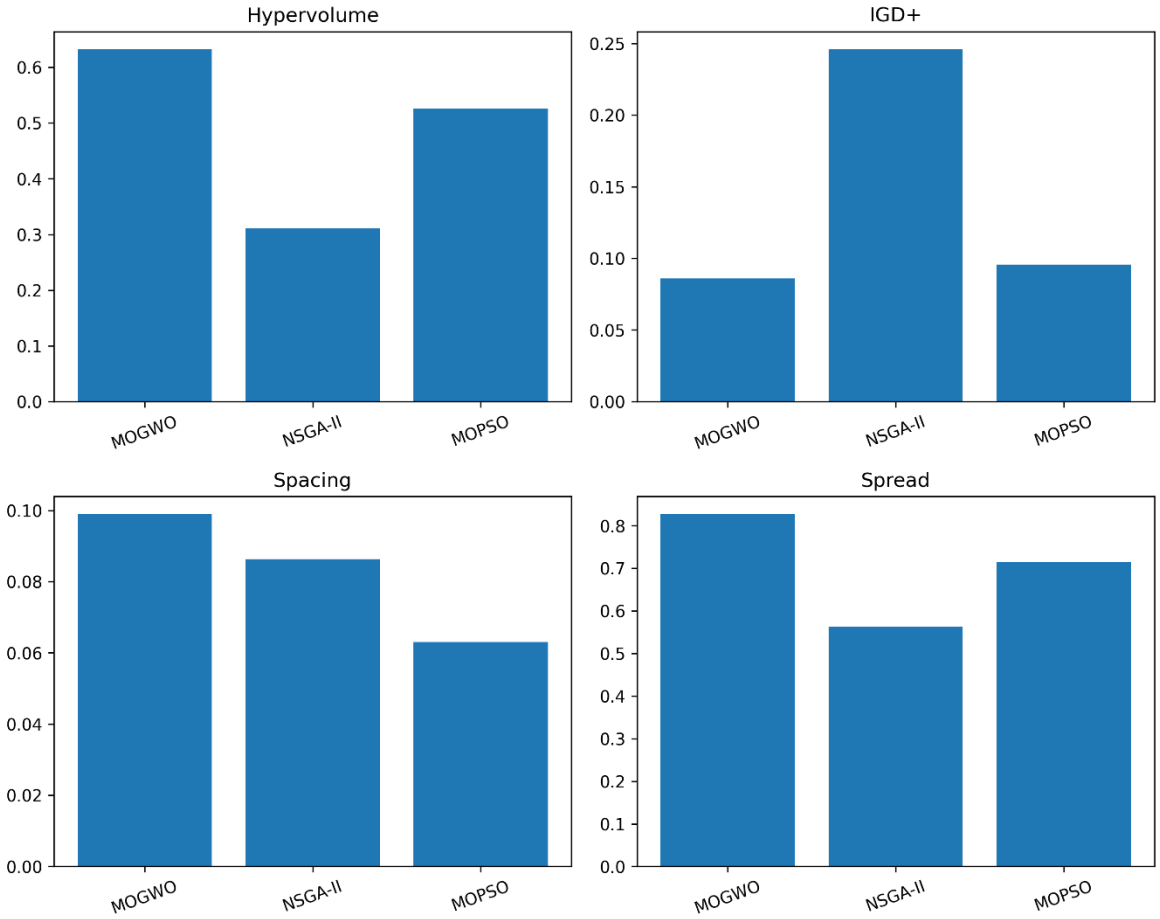

Fig. 4 Comparative results on three meta-heuristics methods based on HV, IGD+, Spacing and Spread measures

The preliminary metrics provide favorable evidence for the proposed approach. MOGWO obtained a Hyper volume of 0.6323, which was 103.4% higher than the NSGA-II value and 20.3% higher than the MOPSO value. Its IGD+ value of 0.0861 was 65.0% lower than that of NSGA-II and 10.1% lower than that of MOPSO, indicating that the MOGWO approximation was closest to the common reference front. MOGWO also achieved the largest Spread value, exceeding NSGA-II by 47.0% and MOPSO by 15.9%. These three indicators jointly support the conclusion that MOGWO provided the strongest combination of convergence and objective-space coverage in the verified run.

The comparison is not uniformly favorable on every indicator, which strengthens rather than weakens the interpretation. MOPSO achieved the lowest Spacing value and retained 19 feasible solutions, compared with 17 for MOGWO and 6 for NSGA-II. Thus, MOPSO produced the most uniform local spacing, while MOGWO produced the best global coverage and reference-front proximity. NSGA-II found the lowest observed cost extreme, but its lower Hyper volume, higher IGD+, smaller Spread, and small archive indicate that this extreme did not translate into a strong approximation of the full decision surface. Since the proposed problem is explicitly multi-objective, set-level quality is more informative than the best value of any single objective. The evidence therefore points to MOGWO as the most useful decision-support method in this run, while acknowledging MOPSO's advantage in local uniformity.

[Downloaded from mail.ijaor.ir on 2026-11-25]

4.4 Convergence behavior

Figure 5 shows that all algorithms discovered feasible solutions early and improved at least one objective during the six-generation verification run. NSGA-II rapidly reduced the extreme cost value, whereas MOGWO achieved the lowest extreme ARL1 by the fifth generation. MOPSO improved both tracked extremes more gradually. These curves should not be interpreted as a complete ranking because each panel follows only one extreme member of a multi-objective archive. In particular, the higher best-cost trace of MOGWO does not contradict its superior Hyper volume: MOGWO retained solutions across a wider range of ARL0 and ARL1 values instead of concentrating only on the cost-minimizing boundary. The simultaneous use of convergence curves and set-quality indicators is therefore essential for a correct interpretation.

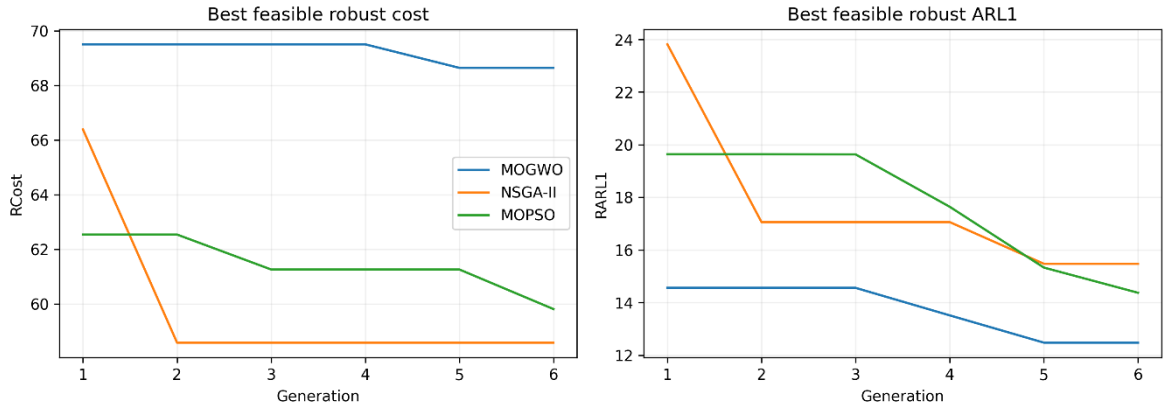

Fig. 5 Comparative evaluation of three methods based on evolution rate of feasible robust cost and feasible robust ARL1

4.5 Comparative study among economic, economic-statistical results

Four representative policies were selected from the MOGWO archive and re-evaluated using the higher-precision validation setting. The economic policy minimizes robust cost, the statistical policy minimizes robust ARL1, the false-alarm-protective policy maximizes robust ARL0, and the balanced policy corresponds to the knee region of the normalized Pareto approximation. All four policies remained feasible after validation, which confirms that the archive was not merely exploiting simulation noise at the statistical boundaries.

Table 4. Validated representative MOGWO monitoring policies

Policy	n	h	L	r	RCost	RARL0	RARL1	Delay	Feas.
Economic	19	8.925	0.999	0.0568	67.045	336.70	13.80	120.35	Yes
Statistical	20	10.193	0.940	0.0587	67.431	247.48	12.14	120.83	Yes
False-alarm protective	19	9.658	1.312	0.0703	79.645	826.37	22.61	211.33	Yes
Balanced knee	20	9.023	1.153	0.0704	70.691	541.36	17.07	150.83	Yes

The economic policy achieved the smallest validated robust cost, 67.045, with RARL0 = 336.70 and RARL1 = 13.80. The statistical policy reduced RARL1 by approximately 12.0% relative to the economic policy while increasing cost by only 0.58%; however, this

[Downloaded from mail.ijaor.ir on 2026-11-25]

improvement reduced RARL0 by 26.5%, indicating weaker protection against false alarms. The false-alarm-protective policy increased RARL0 to 826.37, which was 145.4% above the economic policy, but required an 18.8% increase in robust cost and a 63.9% increase in RARL1.

The balanced knee policy provides the most interpretable compromise. Relative to the economic policy, it increased robust cost by only 5.44% while increasing RARL0 by 60.8%. The associated RARL1 increased by 23.7%, but remained far below the maximum admissible value of 50 for the aggregate response and all cause-specific constraints remained satisfied. The policy therefore offers a substantial reduction in false-alarm exposure for a moderate economic premium, without moving into the highly conservative region represented by the false-alarm-protective policy. This pattern is precisely the type of trade-off that cannot be revealed by a single-objective cost model.

The selected values also provide practical insight into the design variables. All representative policies used relatively large samples, n=19 or 20, and small EWMA smoothing parameters, approximately 0.057-0.070. The large sample sizes improve estimation of the four polynomial coefficients, while the small smoothing parameters preserve memory and increase sensitivity to persistent small changes. The main distinction among policies is therefore created by the combination of the sampling interval and control-limit multiplier: the statistical policy uses the smallest L, whereas the false-alarm-protective policy uses the largest L. This behavior is consistent with the expected role of the control limit in balancing false alarms against detection delay.

4.6 Cost components analysis

Figure 6 and Table 5 show that out-of-control production loss is the dominant economic component for every representative policy. Its share ranges from approximately 70.2% for the economic policy to 77.3% for the false-alarm-protective policy. Sampling is the second-largest component, accounting for approximately 12.4-15.6% of the component total, whereas the direct false-alarm cost contributes less than 0.3%. This decomposition explains an initially counterintuitive result: maximizing ARL0 does not necessarily minimize total cost. The false-alarm-protective policy reduces the already small false-alarm component, but its slower detection substantially increases out-of-control loss. The economic optimum is therefore governed primarily by the interaction between sampling effort and undetected out-of-control operation, not by false-alarm cost alone.

Table 5 Decomposition of cost function values in different policies

Policy	In-control	Out-of-control	False alarm	Repair	Sampling	Component total
Economic	6.177	45.522	0.131	2.904	10.108	64.843
Statistical	6.267	44.898	0.162	2.931	9.248	63.507
False-alarm protective	5.268	58.347	0.044	2.463	9.381	75.502
Balanced knee	5.888	48.944	0.035	2.764	10.403	68.033

[Downloaded from mail.ijaor.ir on 2026-11-25]

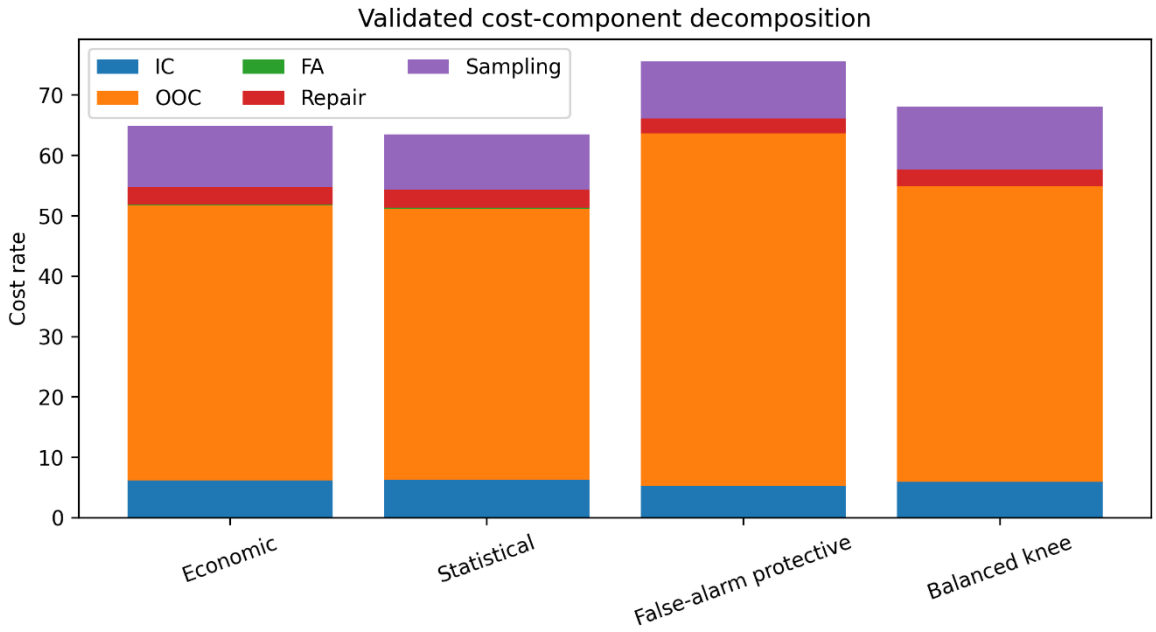

Fig. 6 Decomposition of the validated and optimized cost into In-Control (IC), False Alarm (FA), Sampling, Out-of-Control (OOC) and Repair cost.

This result is consistent with recent economic-statistical studies showing that realistic memory-type models can be dominated by out-of-control loss and that overly simplified cost expressions may understate the economic effect of detection delay [28-39]. The proposed approach strengthens this line of research by calculating cost directly from the simulated production cycle and by preserving cause-specific differences in failure rates, shifts, and repair consequences. The component analysis also provides managerial transparency: reductions in the largest component can be prioritized instead of relying only on the aggregate objective value.

4.7 Sensitivity and robustness analysis

A one-at-a-time sensitivity analysis was conducted around the balanced knee policy by changing the out-of-control cost C1, false-alarm cost F, repair cost W, process standard deviation, and shift magnitude by ±20%. The policy itself was held fixed so that the resulting changes reflect parameter sensitivity rather than re-optimization. This distinction is important because the analysis evaluates the robustness of an implemented policy after the operating environment changes.

[Downloaded from mail.ijaor.ir on 2026-11-25]

Table 6 Sensitivity analysis on the main cost function and control chart parameters

Parameter	Change	RCost	RARL0	RARL1	ΔCost (%)	ΔARL0 (%)	ΔARL1 (%)
C1	-20%	60.319	541.36	17.07	-14.67	+0.00	+0.00
C1	+20%	81.063	541.36	17.07	+14.67	+0.00	+0.00
F	-20%	70.684	541.36	17.07	-0.01	+0.00	+0.00
F	+20%	70.699	541.36	17.07	+0.01	+0.00	+0.00
W	-20%	70.122	541.36	17.07	-0.81	+0.00	+0.00
W	+20%	71.261	541.36	17.07	+0.81	+0.00	+0.00
sigma	-20%	76.496	1164.81	22.97	+8.21	+115.17	+34.58
sigma	+20%	64.323	111.68	12.02	-9.01	-79.37	-29.62
shift	-20%	84.456	541.36	25.99	+19.47	+0.00	+52.24
shift	+20%	63.341	541.36	11.86	-10.40	+0.00	-30.52

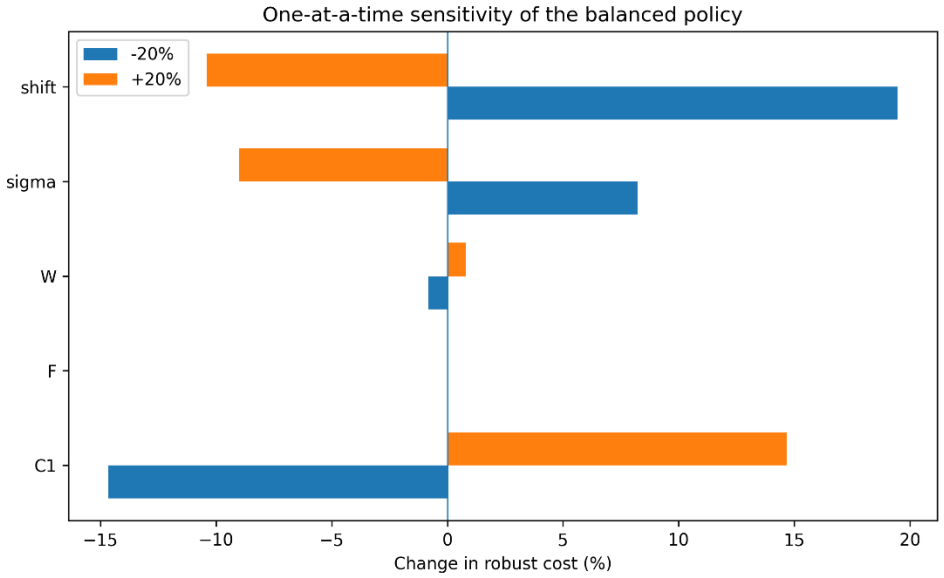

Fig. 7 Results of the impact of main parameters changes on the robust costs and statistical measures

The sensitivity results identify three dominant drivers. First, a ±20% change in the out-of-control cost produced an approximately symmetric ±14.67% change in robust cost, without affecting the run-length measures because only the economic consequences changed. Second, shift magnitude had the strongest joint economic-statistical effect: a 20% reduction increased RARL1 by 52.24% and robust cost by 19.47%, whereas a 20% increase reduced RARL1 by 30.52% and robust cost by 10.40%. This confirms that difficult-to-detect small shifts are economically important even when the direct cost parameters remain unchanged.

Third, process standard deviation produced the largest change in false-alarm behavior. A 20% reduction in sigma increased RARL0 by 115.17% and increased RARL1 by 34.58%, whereas a 20% increase reduced RARL0 by 79.37% and reduced RARL1 by 29.62%. This apparently asymmetric behavior follows from the use of the fixed Phase-I covariance matrix: changes in actual dispersion alter the scale of the incoming coefficient estimates relative to the reference distribution. The result is methodologically important because it demonstrates that uncertainty in process dispersion cannot be treated as a harmless nuisance parameter. In contrast, the false-alarm cost F had almost no effect on the total robust cost, and the repair cost W produced changes below 1%, which is consistent with the cost decomposition in the Cost-Component Analysis subsection.

[Downloaded from mail.ijaor.ir on 2026-11-25]

4.8 Discussion and comparison with prior literature

Discussion should focus on methodological scope rather than raw cost values because previous studies use different cost scales, shift structures, and simulation assumptions. Relative to Williams et al. [32], which established statistical monitoring for nonlinear profiles, the present framework adds economic objectives, competing assignable causes, and scenario-based uncertainty. Relative to the linear-profile economic-statistical designs of Roshanbin et al. [22], Ershadi et al. [4], and Shojaee et al. [39], the model extends the monitored relationship to a nonlinear polynomial coefficient vector and retains a fixed Phase-I reference while process conditions vary. Recent memory-type and production-maintenance studies [28, 24, 29] support the importance of explicitly modeling multiple causes and delayed economic consequences; the present cost decomposition is consistent with that direction, particularly in showing the practical importance of out-of-control loss.

The algorithmic findings are also consistent with the multi-objective literature in a qualified sense. MOGWO's archive and multi-leader mechanism [16] and [19] is designed to preserve diverse non-dominated alternatives, and the verified run exhibits broader objective-space coverage and better observed HV/IGD+ values than the two comparators, whereas MOPSO shows better local spacing and NSGA-II reaches a competitive low-cost extreme. Recent two-archive MOGWO work similarly emphasizes convergence-diversity balance [31]. Because only one independent run is retained here, these observations are descriptive; they support the plausibility of the proposed search strategy but not an inferential claim of universal algorithmic superiority.

From a decision-making perspective, the study contributes more than a single best design. The representative policies quantify the price of faster detection or stronger false-alarm protection, while the sensitivity analysis identifies out-of-control cost, process dispersion, and shift magnitude as the parameters most deserving of accurate estimation. This interpretation is aligned with recent economic-statistical studies [8, 9, 13, 21, 25, 26, 28, 30, 39] which increasingly treat monitoring as a joint statistical and operational decision. The practical implication is that managers can choose a policy according to risk tolerance and operating conditions rather than being forced into one cost-minimizing setting.

5 Conclusion

This study developed a robust multi-objective economic-statistical approach for monitoring nonlinear quality profiles under parameter uncertainty and multiple assignable causes. The proposed approach integrates a third-order polynomial profile, Phase I estimation of a fixed reference mean and covariance matrix, an EWMA-Hotelling T^2 statistic, cause-specific competing risks, direct Monte Carlo estimation of run-length behavior, regenerative-cycle cost simulation, and scenario-based robustness. The four design variables sample size, sampling interval, control-limit multiplier, and EWMA smoothing parameter are optimized simultaneously with respect to robust cost, robust in-control protection, and robust out-of-control detection performance. The computational evaluation showed that the contribution is broader than replacing NSGA-II with another metaheuristic. Under the common preliminary evaluation budget, MOGWO generated the highest Hyper volume, the lowest IGD+, and the widest Spread, indicating the strongest combination of global convergence and objective-space coverage among the three compared algorithms. MOPSO achieved the most uniform local spacing, and NSGA-II reached a competitive low-cost extreme; therefore, no algorithm

[Downloaded from mail.ijaor.ir on 2026-11-25]

dominated every scalar indicator. The principal advantage of MOGWO was the production of a more comprehensive decision set from which economically efficient, statistically sensitive, false-alarm-protective, and balanced knee policies could be selected. These algorithmic comparisons should be interpreted as descriptive evidence from the retained verification run until the planned repeated-run statistical analysis is completed.

The representative-policy and cost-component analyses provided practical insight into the economic-statistical trade-offs. The balanced knee policy increased robust cost by only 5.44% relative to the economic policy while increasing robust ARL_0 by 60.8%, thereby substantially strengthening false-alarm protection without entering the highly conservative region. Out-of-control production loss remained the dominant cost component, which explains why maximizing ARL_0 alone did not minimize total cost. Sensitivity analysis further showed that shift magnitude, process dispersion, and out-of-control cost deserve the greatest estimation and managerial attention, whereas direct false-alarm and repair costs had comparatively smaller effects in the examined setting. The study has several limitations. The available comparative evidence was generated from one verified run per algorithm with a deliberately small verification budget, three uncertainty scenarios, synthetic polynomial profiles, normally distributed errors, and a fixed Phase I covariance matrix. Consequently, the numerical results establish implementation consistency and favorable descriptive performance but do not constitute a definitive statistical ranking. In addition, the model assumes that only the first competing assignable cause remains active within a regenerative cycle and that profile structure is correctly specified.

Future research should complete the planned 30-run confirmatory experiment with matched random seeds and corrected pairwise tests, examine real industrial profile data, and study nonparametric, generalized, functional, and multimode profiles. Adaptive EWMA schemes that adjust the smoothing parameter in response to estimated shift magnitude offer a natural extension [1]. Joint production-maintenance formulations with multiple assignable causes may also strengthen the economic realism of the cycle model [24]. Finally, enhanced MOGWO variants, including recent dual-archive designs that explicitly separate exploration and exploitation, provide a promising direction for improving diversity and convergence in larger or noisier versions of the problem [31].

References

1. AlQadi, H., Abdelfattah, W., Abbas, T., Ahmadini, A. A. H., Sayed, A. I. A., & Ahmad, B. (2025). Design of an EWMA control chart by adaptation of smoothing constant based on a function of estimated shift. Scientific Reports, 15, Article 24730. https://doi.org/10.1038/s41598-025-09735-z
2. Capezza, C., Centofanti, F., Lepore, A., Palumbo, B., & Vantini, S. (2024). Robust multivariate functional control chart. Technometrics, 66(4), 531-547. https://doi.org/10.1080/00401706.2024.2327346
3. Demsar, J. (2006). Statistical comparisons of classifiers over multiple data sets. Journal of Machine Learning Research, 7, 1-30.
4. Ershadi, M. J., Ershadi, M. M., Haghighi Naeini, S., & Niaki, S. T. A. (2021). An economic-statistical design of simple linear profiles with multiple assignable causes using a combination of MOPSO and RSM. Soft Computing, 25, 11087-11100. https://doi.org/10.1007/s00500-021-05854-7
5. Haridy, S., Alamassi, B., Maged, A., Shamsuzzaman, M., Al Owad, A., & Bashir, H. (2023). Economic statistical model of the np chart for monitoring defectives. Scientific Reports, 13, Article 13179. https://doi.org/10.1038/s41598-023-40151-3
6. Hotelling, H. (1947). Multivariate quality control. In C. Eisenhart, M. W. Hastay, & W. A. Wallis (Eds.), Techniques of Statistical Analysis (pp. 111-184). McGraw-Hill.
7. Ishibuchi, H., Masuda, H., Tanigaki, Y., & Nojima, Y. (2015). Modified distance calculation in generational distance and inverted generational distance. In A. Gaspar-Cunha, C. Henggeler Antunes, & C.

[Downloaded from mail.ijaor.ir on 2026-11-25]

Coello Coello (Eds.), Evolutionary Multi-Criterion Optimization (pp. 110-125). Springer. https://doi.org/10.1007/978-3-319-15892-1_8
8. Jafarian-Namin, S., Fattahi, P., & Salmasnia, A. (2025). Assessing the economic-statistical performance of variable acceptance sampling plans based on loss function. Computational Statistics, 40(7), 3665-3713. https://doi.org/10.1007/s00180-024-01581-3
9. Jafarian-Namin, S., Fattahi, P., & Amjad, F. (2026). Optimizing single-objective and bi-objective models for economic-statistical design of RGS plan using particle swarm optimization. Communications in Statistics-Simulation and Computation. Advance online publication. https://doi.org/10.1080/03610918.2026.2617287
10. Jalilibal, Z., Amiri, A., & Khoo, M. B. C. (2022). A literature review on joint control schemes in statistical process monitoring. Quality and Reliability Engineering International, 38(6), 3270-3289. https://doi.org/10.1002/qre.3114
11. Jalilibal, Z., Ahmadi Karavigh, M. H., Amiri, A., & Khoo, M. B. C. (2023). Run rules schemes for statistical process monitoring: A literature review. Quality Technology & Quantitative Management, 20(1), 21-52. https://doi.org/10.1080/16843703.2022.2084281
12. Kang, L., & Albin, S. L. (2000). On-line monitoring when the process yields a linear profile. Journal of Quality Technology, 32(4), 418-426. https://doi.org/10.1080/00224065.2000.11980027
13. Lee, M. H., Khoo, M. B. C., Haq, A., & Chew, X. Y. (2023). Economic-statistical design of the variable sampling interval Poisson EWMA chart. Communications in Statistics-Simulation and Computation, 52(5), 2139-2150. https://doi.org/10.1080/03610918.2021.1898637
14. Lorenzen, T. J., & Vance, L. C. (1986). The economic design of control charts: A unified approach. Technometrics, 28(1), 3-10. https://doi.org/10.1080/00401706.1986.10488092
15. Lowry, C. A., Woodall, W. H., Champ, C. W., & Rigdon, S. E. (1992). A multivariate exponentially weighted moving average control chart. Technometrics, 34(1), 46-53. https://doi.org/10.1080/00401706.1992.10485232
16. Makhadmeh, S. N., Alomari, O. A., Mirjalili, S., Al-Betar, M. A., & Elnagar, A. (2022). Recent advances in multi-objective grey wolf optimizer, its versions and applications. Neural Computing and Applications, 34(22), 19723-19749. https://doi.org/10.1007/s00521-022-07704-5
17. Maleki, M. R., Amiri, A., & Castagliola, P. (2018). An overview on recent profile monitoring papers (2008-2018) based on a conceptual classification scheme. Computers & Industrial Engineering, 126, 705-728. https://doi.org/10.1016/j.cie.2018.10.008
18. Mirjalili, S., Mirjalili, S. M., & Lewis, A. (2014). Grey Wolf Optimizer. Advances in Engineering Software, 69, 46-61. https://doi.org/10.1016/j.advengsoft.2013.12.007
19. Mirjalili, S., Saremi, S., Mirjalili, S. M., & Coelho, L. S. (2016). Multi-objective grey wolf optimizer: A novel algorithm for multi-criterion optimization. Expert Systems with Applications, 47, 106-119. https://doi.org/10.1016/j.eswa.2015.10.039
20. Motsepa, C. M., Malela-Majika, J. C., Castagliola, P., & Shongwe, S. C. (2023). Double sampling monitoring schemes: A literature review and some future research ideas. Communications in Statistics-Simulation and Computation, 52(8), 3391-3419. https://doi.org/10.1080/03610918.2021.1939375
21. Nasiri Pour, A., Azizi, A., Rahimzadeh, A., Ershadi, M. J., & Zeinalnezhad, M. (2024). Designing a log-logistic-based EWMA control chart using MOPSO and VIKOR approaches for monitoring cardiac surgery performance. Decision Making: Applications in Management and Engineering, 7(1), 342-363. https://doi.org/10.31181/dmame712024903
22. Roshanbin, N., Ershadi, M. J., & Niaki, S. T. A. (2022). Multi-objective economic-statistical design of simple linear profiles using a combination of NSGA-II, RSM, and TOPSIS. Communications in Statistics-Simulation and Computation, 51(4), 1704-1720. https://doi.org/10.1080/03610918.2019.1680692
23. Sabahno, H., & Amiri, A. (2023). New statistical and machine learning based control charts with variable parameters for monitoring generalized linear model profiles. Computers & Industrial Engineering, 184, Article 109562. https://doi.org/10.1016/j.cie.2023.109562
24. Salmasnia, A., Dehghani, S., & Sharafi, S. (2025). Economic-statistical design of ARMA chart for an integrated production and maintenance model in presence of multiple assignable causes, rework process, and random failures. International Journal of System Assurance Engineering and Management, 16(9), 2983-3001. https://doi.org/10.1007/s13198-025-02803-7
25. Sandeep, & Mukhopadhyay, A. R. (2025a). Double-objective economic statistical design of the u-chart: NSGA II approach. Journal of Statistical Computation and Simulation, 95(5), 1091-1109. https://doi.org/10.1080/00949655.2024.2446382

[Downloaded from mail.ijaor.ir on 2026-11-25]

26. Sandeep, & Mukhopadhyay, A. R. (2025b). The multi-objective economic statistical design of the p-chart: NSGA II approach. Communications in Statistics-Simulation and Computation, 54(12), 4995-5012. https://doi.org/10.1080/03610918.2024.2423876
27. Saniga, E. M. (1989). Economic statistical control-chart designs with an application to X-bar and R charts. Technometrics, 31(3), 313-320. https://doi.org/10.1080/00401706.1989.10488554
28. Shiravani, F., Bameni Moghaddam, M., & Pourtaheri, R. (2026). Optimized realistic economic-statistical design of memory-type control charts with Burr type XII shock model for multiple independent assignable causes. Quality & Quantity, 60(3), 9101-9136. https://doi.org/10.1007/s11135-026-02622-3
29. Shojaee, M., Noori, S., Jafarian-Namin, S., Hassanvand, F., & Johannssen, A. (2024a). Designing economic-statistical Hotelling's T^2 control charts for monitoring linear profiles under uncertainty of parameters. Journal of Statistical Computation and Simulation, 94(18), 4019-4036. https://doi.org/10.1080/00949655.2024.2408365
30. Shojaee, M., Noori, S., Jafarian-Namin, S., & Johannssen, A. (2024b). Integration of production-maintenance planning and monitoring simple linear profiles via Hotelling's T^2 control chart and particle swarm optimization. Computers & Industrial Engineering, 188, Article 109864. https://doi.org/10.1016/j.cie.2023.109864
31. Tejani, G. G., Sharma, S. K., Mousavirad, S. J., & Radwan, A. (2025). The two-archive multi-objective grey wolf optimization algorithm for truss structures. International Journal of Computational Intelligence Systems, 18, Article 245. https://doi.org/10.1007/s44196-025-00972-8
32. Williams, J. D., Woodall, W. H., & Birch, J. B. (2007). Statistical monitoring of nonlinear product and process quality profiles. Quality and Reliability Engineering International, 23(8), 925-941. https://doi.org/10.1002/qre.858
33. Woodall, W. H., Spitzner, D. J., Montgomery, D. C., & Gupta, S. (2004). Using control charts to monitor process and product quality profiles. Journal of Quality Technology, 36(3), 309-320. https://doi.org/10.1080/00224065.2004.11980276
34. Zitzler, E., & Thiele, L. (1999). Multiobjective evolutionary algorithms: A comparative case study and the strength Pareto approach. IEEE Transactions on Evolutionary Computation, 3(4), 257-271. https://doi.org/10.1109/4235.797969

[Downloaded from mail.ijaor.ir on 2026-11-25]